

# Beta-Delayed Proton Emission Branches in $^{43}\text{Cr}$

M. Pomorski,<sup>1</sup> K. Miernik,<sup>1</sup> W. Dominik,<sup>1</sup> Z. Janas,<sup>1</sup> M. Pfützner,<sup>1,\*</sup> C.R. Bingham,<sup>2</sup>  
H. Czyrkowski,<sup>1</sup> M. Ćwiok,<sup>1</sup> I.G. Darby,<sup>2</sup> R. Dąbrowski,<sup>1</sup> T. Ginter,<sup>3</sup> R. Grzywacz,<sup>2,4</sup> M. Karny,<sup>1</sup>  
A. Korgul,<sup>1</sup> W. Kuśmierz,<sup>1</sup> S.N. Liddick,<sup>2</sup> M. Rajabali,<sup>2</sup> K. Rykaczewski,<sup>4</sup> and A. Stolz<sup>3</sup>

<sup>1</sup>*Faculty of Physics, University of Warsaw, 00-681 Warsaw, Poland*

<sup>2</sup>*Department of Physics and Astronomy, University of Tennessee, Knoxville, TN 37996, USA*

<sup>3</sup>*National Superconducting Cyclotron Laboratory, Michigan State University, East Lansing, MI 48824, USA*

<sup>4</sup>*Physics Division, Oak Ridge National Laboratory, Oak Ridge, TN 37831, USA*

(Dated: December 22, 2010)

The  $\beta^+$  decay of very neutron deficient  $^{43}\text{Cr}$  has been studied by means of an imaging time projection chamber which allowed recording tracks of charged particles. Events of  $\beta$ -delayed emission of one-, two-, and three protons were clearly identified. The absolute branching ratios for these channels were determined to be  $(81 \pm 4)\%$ ,  $(7.1 \pm 0.4)\%$ , and  $(0.08 \pm 0.03)\%$ , respectively. The  $^{43}\text{Cr}$  is thus established as the second case in which the  $\beta$ - $3p$  decay occurs. Although the feeding to the proton-bound states in  $^{43}\text{V}$  is expected to be negligible, the large branching ratio of  $(12 \pm 4)\%$  for decays without proton emission is found.

PACS numbers: 23.90.+w, 27.40.+z, 29.40.Cs, 29.40.Gx

The  $\beta$ -delayed emission of protons is a characteristic feature of very neutron deficient nuclei which have large decay energies and thus substantial probability of  $\beta$  transitions feeding highly excited and particle-unbound states in daughter nuclei. Since the first observation of delayed proton emission, almost 50 years ago [1], such decays provided a wealth of information on structure of neutron-deficient nuclei far from stability, providing tests to nuclear models and yielding data needed for the understanding of the astrophysical  $rp$ -process [2]. With the progress in experimental techniques more exotic systems could be reached and the phenomena of  $\beta$ -delayed multiparticle emission become open to investigation. The  $\beta$ -delayed two-proton decay was observed for the first time in 1983 in the decays of  $^{22}\text{Al}$  and  $^{26}\text{P}$  [3, 4]. Later, several other cases of such decay mode were identified [5].

A few years ago, we have communicated the first observation of  $\beta$ -delayed three-proton emission, which was found in the decay of  $^{45}\text{Fe}$  [6]. The identification of this new channel was possible due to application of a new type of ionization chamber, equipped with optical readout — called the Optical Time Projection Chamber (OTPC) — which was developed to study in detail the two-proton ( $2p$ ) radioactivity of  $^{45}\text{Fe}$  [7, 8]. This detector proved to be extremely sensitive, yielding clear and unambiguous images of decays of single atoms stopped within its volume. The evidence of the  $3p$  channel following  $\beta^+$  decay of  $^{45}\text{Fe}$  was based on four events [6]. In the same experiment, as a byproduct, information on the  $\beta^+$  decay of  $^{43}\text{Cr}$  was collected as well. In this Rapid Communication, we present results obtained for the decay of  $^{43}\text{Cr}$ , which include evidence for the  $\beta$ - $3p$  decay channel.

The first observation of  $^{43}\text{Cr}$  and the first determination on its decay properties were achieved in 1992 by

Borrel et al. using the LISE separator at GANIL and the technique of implantation into silicon detectors for spectroscopic studies [9]. Later more detailed work was devoted to  $^{43}\text{Cr}$  at this laboratory and all results are summarized in a recent paper by Dossat et al. [10]. The half-life was found to be  $T_{1/2} = (21.1 \pm 0.4)$  ms. Several  $\beta$ -delayed proton branches as well as one  $\beta$ -delayed two-proton channel were identified. The total probability for emission of protons in the decay of  $^{43}\text{Cr}$  was determined to be  $92.5(28)\%$  [10]. Such large value is expected, since the  $\beta$ -daughter nucleus,  $^{43}\text{V}$  is weakly bound — according to the systematics of Audi et al. its proton separation energy is predicted to be  $S_p = 190(230)$  keV [11]. From the same systematics, the decay energy of  $^{43}\text{Cr}$  is estimated to be  $Q_{EC} = 15.9 \pm 0.2$  MeV. In the work of Dossat et al., the total branching ratio for emission of protons was deduced from the decay-time analysis of the total charged-particle spectrum, with somewhat arbitrary assumptions on the threshold energy and a contribution from  $\beta$  particles [10]. Such a procedure was necessary because not all proton-emission channels could be identified as lines in the spectrum. For the same reason, no absolute branching ratios could be determined separately for  $\beta$ - $p$  and  $\beta$ - $2p$  channels. No evidence for the  $\beta$ - $3p$  transitions was observed.

When  $^{45}\text{Fe}$  undergoes the  $2p$  radioactivity it transforms into  $^{43}\text{Cr}$ , thus the decays of the latter can be observed after implantation of the former. Indeed, in our  $2p$  decay study of  $^{45}\text{Fe}$  we could identify  $\beta$ -delayed proton decay of  $^{43}\text{Cr}$  following the  $2p$  emission from  $^{45}\text{Fe}$  [8]. We recorded 17 events of  $\beta$ - $p$  and two events of  $\beta$ - $2p$  channels. These numbers were found to be consistent with time observation windows imposed on  $^{45}\text{Fe}$  implantation events, with the half-life of the  $^{43}\text{Cr}$ , and with the known branching ratios [10]. However, in the reaction used to produce the ions of  $^{45}\text{Fe}$ , also the  $^{43}\text{Cr}$  ions are produced. Since the mass-to-charge ratio for these two nuclei is similar, and the production cross section for the

\*Electronic address: pfutzner@fuw.edu.pl

$^{43}\text{Cr}$  is much larger, the latter ions are transmitted to a detection apparatus in large quantity offering the possibility to study their decays on their own. In this paper, we focus on decay studies of such primarily produced  $^{43}\text{Cr}$  ions implanted in our detector. We note, that in a different study of  $2p$  radioactivity of  $^{45}\text{Fe}$  performed by Giovinazzo et al. a large number of  $^{43}\text{Cr}$  was implanted as well into a TPC detector used for decay spectroscopy [12]. Their detection of  $\beta$ - $2p$  events represents the first direct observation of the two protons emitted after  $\beta$  decay [12]. However, no detailed branching ratios were extracted, and no evidence for the  $\beta$ - $3p$  decay was found in this work.

Our experiment was performed at the National Superconducting Cyclotron Laboratory at Michigan State University, East Lansing, USA. The experimental details were given already in Refs.[6, 8], here we recall only the most important points. The ions of interest were produced in the fragmentation reaction of a  $^{58}\text{Ni}$  beam at 161 MeV/nucleon, with average intensity of 15 pA, impinging on a 800 mg/cm<sup>2</sup> thick natural nickel target. The products were selected using the A1900 fragment separator [13] and identified in-flight by using time-of-flight (TOF) and energy-loss ( $\Delta E$ ) information for each ion. The TOF was measured between a plastic scintillator located in the middle focal plane of the A1900 separator and a thin silicon detector mounted at the end of the beam-line. The silicon detector also provided the  $\Delta E$  signal. Identified ions were slowed down in an aluminium foil and stopped inside the active volume of the OTPC detector. The acquisition system was triggered only by those ions for which the TOF value exceeded a certain limit. This limit was selected in a way to accept all ions of  $^{45}\text{Fe}$  and a small part of the  $^{43}\text{Cr}$  ions. The rate of triggers due to  $^{43}\text{Cr}$  ions was about 8 events per minute. The identification plot of all ions coming to the counting station was presented in Ref.[8]. Here, in Figure 1 we show the identification spectrum of those ions which triggered the OTPC acquisition system. The total number of  $^{43}\text{Cr}$  events, selected for the further analysis by the gate shown in Figure 1, was about 40000.

The principles of operation of the OTPC detector are following. Ions and their charged decay products were stopped in a volume of  $20 \times 20 \times 42 \text{ cm}^3$  filled with a counting gas at atmospheric pressure. A mixture of helium (66%), argon (32%), nitrogen (1%), and methane (1%) was used. The primary ionization electrons drift in a uniform electric field, with a velocity of  $0.97 \text{ cm}/\mu\text{s}$ , towards a double-stage amplification structure formed by parallel-mesh flat electrodes. In the second multiplication stage, emission of UV photons occurs. After conversion of their wavelength to the visual range by a thin luminescent foil, these photons were recorded by a CCD camera and by a photomultiplier tube (PMT). The camera image represents the projection of particles' tracks on the luminescent foil. The signals from the PMT were sampled with a 50 MHz frequency by a digital oscilloscope yielding the time dependence of the total light intensity. This pro-

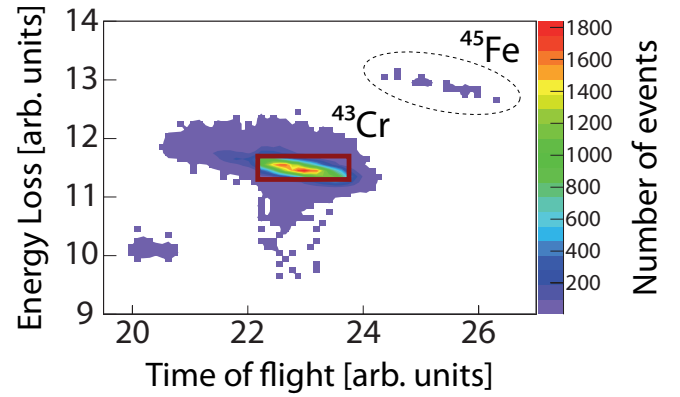


FIG. 1: (Color online) Identification spectrum of ions accepted by the OTPC acquisition system. The gate used to select  $^{43}\text{Cr}$  ions for the further analysis is shown by a brown rectangle.

vides timing information of events and additionally on the drift-time which is related to the position along the axis normal to the image plane. By changing the potential of an auxiliary gating electrode, the chamber can be switched between a low sensitivity mode in which tracks of highly ionizing heavy ions can be recorded, and a high sensitivity mode used to detect light particles emitted during the decay.

For each event, the corresponding CCD image and the PMT time profile, assigned unambiguously to the accepted identified ion, were stored on a computer hard disk. The trigger signal was also used to switch the OTPC to the high sensitivity mode and to turn the beam off for a period of 50 ms to prevent other ions from entering the detector while waiting for the decay of the stopped ion. While the sampling of the PMT signal was always started by the trigger, two different modes of camera operation were used. In the first, the *asynchronous* mode, the CCD was running continuously so that the frames were not correlated with the triggers. The camera exposure time in this mode was 30 ms per frame. Upon arrival of the trigger, the current frame was validated and read-out after the exposure, while neighboring frames were discarded. In this mode the track of the incoming ion was recorded. Since the arrival of the ion occurs randomly within the frame exposure time, the time left for the detection of the decay is different in each case. To avoid this disadvantage, in the second *synchronous* mode, the CCD exposure was started by the trigger signal. The exposure time in this mode was 24 ms. Since the camera could start recording an image only after about  $100 \mu\text{s}$  after the trigger, the track of the incoming heavy ion could not be seen in this mode. On the other hand, the time window for the decay detection was the same for each ion and equal to the camera exposure time. Out of about 40000 selected  $^{43}\text{Cr}$  triggers, about 30000 were collected in the synchronous mode, and about 10000 in the asynchronous one. Since the range distribution of

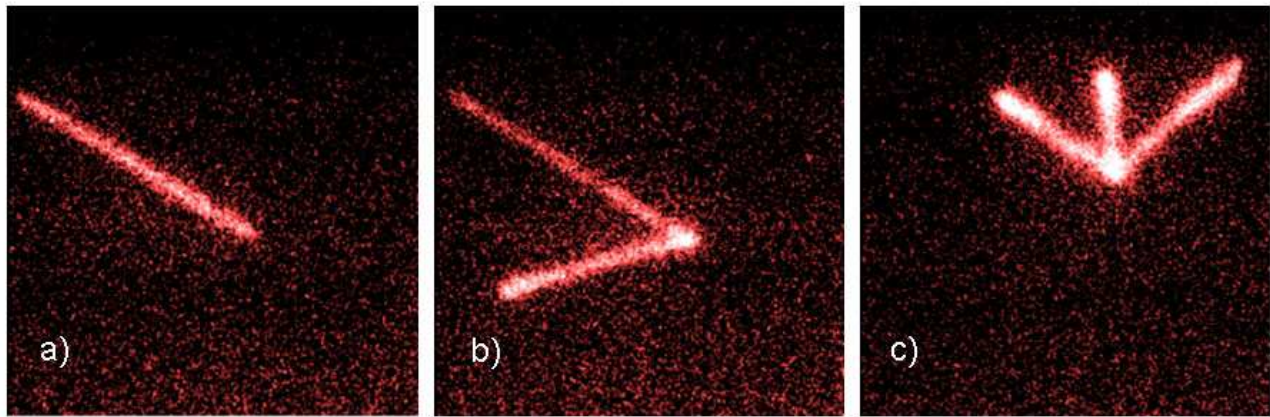


FIG. 2: Example CCD images of  $^{43}\text{Cr}$  decays by  $\beta$ -delayed proton(s) emission, recorded in the synchronous mode in which the track of an incoming ion is not seen. The cases of emission of a single proton (a), two protons (b) and three protons (c) are shown. The ionizing power of the positron is too small to see its trace.

products selected by A1900 separator was larger than the thickness of the OTPC detector, not all ions which triggered the acquisition system were actually stopped within the active part of the chamber. Moreover, the experimental conditions were optimized for ions of  $^{45}\text{Fe}$  which had slightly different range profile. In addition, because the exposure time, also chosen for the decay of  $^{45}\text{Fe}$ , was comparable with the half-life of  $^{43}\text{Cr}$ , a significant fraction of the stopped  $^{43}\text{Cr}$  ions decayed after the exposure was closed. Finally, even if an ion is properly stopped and does decay within the observation time, there is a probability that the decay is not accompanied by  $\beta$ -delayed protons. In such case only the track of the incoming ion will be seen in the asynchronous mode, and nothing will be seen in the synchronous mode, because the ionization power of a positron is too small to leave a trace in the detector.

Among decays collected in the synchronous mode, we have observed 11502 events with emission of a single proton, 1010 events with simultaneous emission of two protons and in 12 events three protons were seen to emerge simultaneously from the decay vertex. Example events from these three categories are shown in Figure 2. The clear and unambiguous images of three-proton emission, like the shown in Figure 2c, establish the  $^{43}\text{Cr}$  as the second nucleus, after  $^{45}\text{Fe}$  [6], in which such decay channel is identified. The numbers of events given above yield the relative branching ratios of 91.8(3)%, 8.1(3)%, and 0.096(30)% for the  $\beta$ -delayed one-, two-, and three-proton emission, respectively. Decay times of events in the synchronous mode, recorded by the PMT tube, allow to extract the half-life of the  $^{43}\text{Cr}$ . The histogram of decay times for all events of  $\beta$ -1p emission observed in this mode is shown in Figure 3. The least-square fit to the data yielded the half-life value of  $T_{1/2} = 20.6 \pm 0.9$  ms, in perfect agreement with the best literature value [10].

In the data collected in the asynchronous mode, we

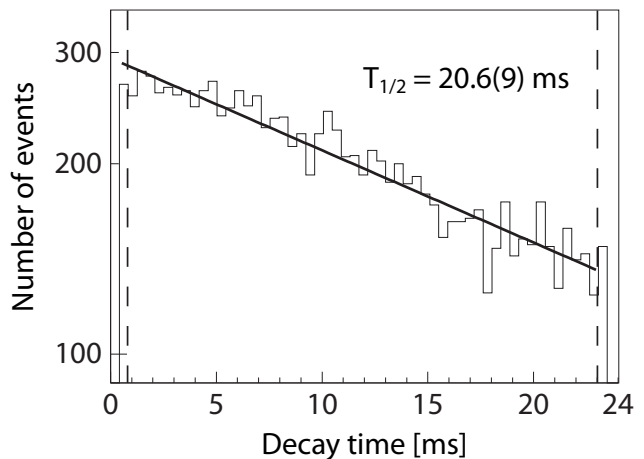


FIG. 3: The histogram shows the decay time distribution of  $^{43}\text{Cr}$  events collected in the synchronous mode. The solid line shows the result of the least-square fit to the data points located between the dashed lines.

found 1663 events of single proton emission, 117 events of two proton emission, and one event of three proton emission, which is consistent with relative branchings deduced from the synchronous mode. In all these events the track of the incoming  $^{43}\text{Cr}$  ion is seen. The  $\beta$ -3p event observed in this mode is shown in Figure 4. In addition, in 4621 events we could see only the heavy ion track, with no decay signal. These events represent cases where either the decay occurred after the exposure time, or the decay without proton emission took place. Since we know the half-life of  $^{43}\text{Cr}$  and the time between the implantation and the end of the exposure for each event (the decay time window), we can calculate the probability that the decay with no protons did occur during such event. Thus, the analysis of events in the asynchronous



mode allows determination of the absolute branching ratios for all decay channels.

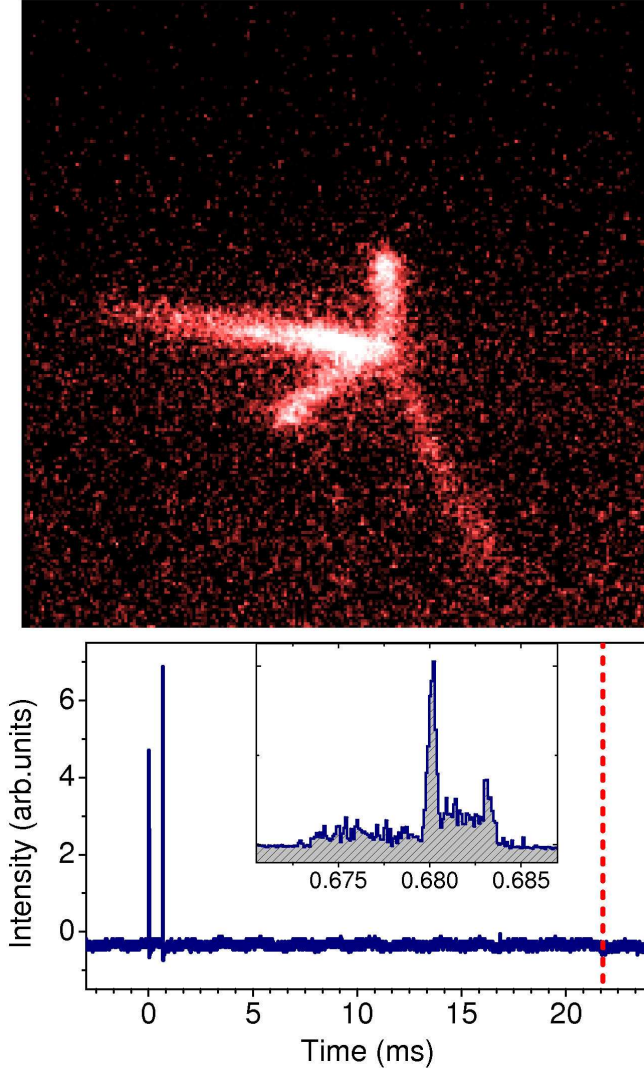


FIG. 4: (Color online) An event of  $\beta$ -delayed three-proton emission from  $^{43}\text{Cr}$  recorded in the asynchronous mode. Top: the CCD image on which a track of a chromium ion entering the detector from the left can be seen. Bottom: the time profile of the total light intensity measured by the PMT. The dashed line indicates the end of the current CCD exposure frame. The clock is started by the implantation of the  $^{43}\text{Cr}$  ion. The decay event occurred 0.68 ms after the implantation and 21.1 ms before the end of the CCD frame. In the inset, the magnified part is plotted, showing in detail the decay event.

If the probability for the  $\beta$  decay with no emission of delayed protons is  $b_0$ , then the likelihood function, defined as the product of probabilities for all events, can be written as

$$\mathcal{L} = \prod_{i=1}^{N_p} [(1 - b_0) (1 - e^{-\lambda\tau_i})] \prod_{j=1}^{N_0} [e^{-\lambda\tau_j} + b_0(1 - e^{-\lambda\tau_j})],$$

TABLE I: The absolute branching ratios for the decay channels of  $^{43}\text{Cr}$  with various number of  $\beta$ -delayed protons. The values with a star (\*) were determined in Ref.[10] for channels which could be identified as lines in the proton spectrum.

Number of protons	Branching ratio	
	This work	Ref.[10]
0	0.12(4)	0.075(3)
1	0.81(4)	0.28(1)*
2	0.071(4)	0.056(7)*
3	0.0008(3)	-

where the first product goes over all  $N_p$  decay events with at least one proton emitted, the second products includes all  $N_0$  events where no delayed protons were seen,  $\lambda$  is the decay constant of  $^{43}\text{Cr}$ , and  $\tau_i$  is the decay time window in the  $i$ -th event. According to the maximum likelihood method, the value of  $b_0$  can be determined by finding the maximum value of the function  $\mathcal{L}$ . This procedure applied to all events accumulated in the asynchronous mode in which the ion was clearly stopped within the active volume yielded the value  $b_0 = 0.12 \pm 0.04$ . Combining this value with the relative probabilities discussed earlier, we arrive at the absolute branching ratios for the various decay branches of  $^{43}\text{Cr}$  which are shown in Table 1. For comparison, the results from Ref.[10] are also given in Table 1. The values for the one- and two-proton emission were taken from Table 9 in Ref.[10], they represent only those transitions which could be identified as peaks in the proton spectrum. Many decay channels are missed in that way which is reflected by the difference between the determined total probability for emission of protons (92.5%) and the sum of identified one- and two-proton contributions. However, the branching ratio for  $\beta$ -2p channel, attributed in Ref.[10] to a transition from the IAS state in  $^{43}\text{V}$  to the ground state of  $^{41}\text{Sc}$ , agrees within error bars with the value determined by us. This may indicate that this transition is the only one with the  $\beta$ -delayed two-proton emission, or at least it dominates this decay channel. Also the two branching ratios for decays with no protons, given in Table 1, agree within experimental accuracy. Thus, the missed channels, i.e. not identified as lines in the proton spectrum in Ref.[10], are predominantly of the  $\beta$ -1p type.

The  $\beta$ -delayed three proton channel is found to be very weak, with the branching below the  $10^{-3}$  level. This may explain why this decay mode was not identified in previous experiments on  $^{43}\text{Cr}$ . Its observation in the present work illustrates the extreme sensitivity of the OTPC detector. In principle a single image would suffice as an evidence for such a rare decay mode. We note also that in this exotic transition a proton-drip line nucleus ( $^{43}\text{Cr}$ ) transforms into a stable and doubly-magic one ( $^{40}\text{Ca}$ ).

The relatively large branching ratio for transitions without  $\beta$ -delayed protons is surprising. It could be expected that it results from strong feeding of the ground state of  $^{43}\text{V}$  and of its first excited states lying sufficiently

close to the proton separation energy for proton emission being suppressed. However, the assumption of isospin symmetry and the known  $\beta$  feedings in the mirror decay of  $^{43}\text{K}$  to  $^{43}\text{Ca}$ , indicate that such an explanation is very unlikely. The ground-state to ground-state transition in  $^{43}\text{K}$  is a first forbidden unique ( $3/2^+ \rightarrow 7/2^-$ ) with  $\log ft = 9.71$  [14]. Such a  $\log ft$  value would correspond to the decay of  $^{43}\text{Cr}$  to the ground state of  $^{43}\text{V}$  with the probability of 0.12% only. The strongest allowed transition in the decay of  $^{43}\text{K}$  to the 990 keV state in  $^{43}\text{Ca}$  has the  $\log ft = 5.57$  which would yield a branching of 2% in the decay of  $^{43}\text{Cr}$ . The summed feeding to the ground state and the first four excited states in  $^{43}\text{Ca}$ , up to the 1394 keV energy, would yield less than 3% branching in the decay of  $^{43}\text{Cr}$  if the mirror symmetry were perfect. Moreover, the  $\beta^+$  transitions to the unbound states are observed to be systematically weaker than the corresponding mirror  $\beta^-$  channels [15, 16], which would rather reduce the expected feeding of states in  $^{43}\text{V}$ . It seems plausible that in addition to possible isospin asymmetry effects and/or a serious discrepancy in the proton separation energy in  $^{43}\text{V}$ , some proton-unbound states fed in the decay of  $^{43}\text{Cr}$  have  $\gamma$ -widths much larger than the proton widths. Such a case of  $\gamma$  transitions winning a competition with the proton emission was observed in the decay of  $^{37}\text{Ca}$  [17]. The same effect was suggested as an explanation of an apparent reduction in the feeding of an unbound state in the decay of  $^{20}\text{Mg}$  [16]. However, to check whether the fast  $\gamma$  transitions do explain the large branching for decays with no  $\beta$ -delayed protons, a study invoking both high-resolution  $\gamma$  and proton spectroscopy would be required.

In summary, we have applied a new type of ionization

chamber, in which the optical imaging technique is used to record tracks of charged particles, to the study of  $^{43}\text{Cr}$   $\beta$  decay. Although the experimental conditions were optimized for the measurement of  $2p$  radioactivity of  $^{45}\text{Fe}$  [8] performed during the same experiment, a large number of  $^{43}\text{Cr}$  ions was implanted in the detector and events associated with their  $\beta^+$ -delayed proton emission could be clearly identified. Among them, thirteen events of  $\beta$ -delayed three-proton emission were recorded. Thus,  $^{43}\text{Cr}$  is established as the second case, after  $^{45}\text{Fe}$  [6], where this exotic decay mode is observed. In most cases the emitted protons had energies large enough to escape from the detector's volume, making the detailed kinematical characterization of the decay impossible. However, the relative, as well as the absolute branching ratios for decays with different number of delayed protons could be directly determined. A large branching ratio of  $(12 \pm 4)\%$  was found for decays with no  $\beta$ -delayed protons, although the feeding of proton-bound states in the one-proton daughter nucleus  $^{43}\text{V}$  is expected to be very small by isospin symmetry arguments. Such large value could result from the proton separation energy in  $^{43}\text{V}$  being larger than expected from systematics [11], from substantial isospin asymmetry effects, and from large  $\gamma$ -widths of some proton-unbound states in  $^{43}\text{V}$ .

This work was supported by a grant from the Polish Ministry of Science and Higher Education number 1 P03B 138 30, the U.S. National Science Foundation under grant number PHY-06-06007, and the U.S. Department of Energy under contracts DE-FG02-96ER40983, DEFC03-03NA00143, and DOE-AC05-00OR22725. A.K. acknowledges the support from the Foundation for Polish Science.

- 
- [1] R. Barton, et al., Can. J. Phys. **41**, 2007 (1963).
  - [2] B. Blank and M.J.G. Borge, Prog. Par. Nuc. Phys. **60**, 403 (2008).
  - [3] M.D. Cable et al., Phys. Rev. Lett. **50**, 404 (1983).
  - [4] J. Honkanen et al., Phys. Lett. B **133**, 146 (1983).
  - [5] H.O.U. Fynbo et al., Nucl. Phys. A **677**, 38 (2000).
  - [6] K. Miernik et al., Phys. Rev. C **76**, 041304(R) (2007).
  - [7] K. Miernik et al., Nucl. Instr. and Methods A **581**, 194 (2007).
  - [8] K. Miernik et al. Eur. Phys. J. A **42**, 431 (2009).
  - [9] V. Borrel et al., Z. Phys. A **344**, 135 (1992).
  - [10] C. Dossat et al., Nucl. Phys. A **792**, 18 (2007).
  - [11] G. Audi, O. Bersillon, J. Blachot, A.H. Wapstra, Nucl. Phys. A **729**, 3 (2003).
  - [12] J. Giovinazzo et al., Phys. Rev. Lett. **99**, 102501 (2007).
  - [13] D.J. Morrissey, B.M. Sherill, M. Steiner, A. Stolz and I. Wiedenhoever, Nucl. Instr. Methods in Phys. Res. B **204**, 90 (2003).
  - [14] E.K. Warburton and D.E. Alburger, Phys. Rev. C **38**, 2822 (1988).
  - [15] M.J.G. Borge et al., Phys. Lett. B **317**, 25 (1993).
  - [16] A. Piechaczek et al., Nucl. Phys A **584**, 509 (1995).
  - [17] W. Trinder et al., Nucl. Phys. A **620**, 191 (1997).